Diploptene $\delta^{13}C$ values from contemporary thermokarst lake sediments show complex spatial variation

K. L. Davies[1]*, R. D. Pancost[2,3], M. E. Edwards[4], K. M. Walter Anthony[5], P. G. Langdon[4] and L. Chaves Torres[2]

[1] School of Geography, Earth and Environmental Sciences, Plymouth University, PL4 8AA, United Kingdom

[2] Organic Geochemistry Unit, School of Chemistry, University of Bristol, BS8 1TS, United Kingdom

[3] Cabot Institute, University of Bristol, BS8 1UJ, United Kingdom

[4] Geography & Environment, University of Southampton, SO17 1BJ, United Kingdom

[5] Water & Environment Research Centre, University of Alaska Fairbanks, Fairbanks, Alaska, 99775, USA

*Correspondence to: Kimberley Davies, Kimberley.davies@plymouth.ac.uk

Abstract

Cryospheric changes in northern high latitudes are linked to significant greenhouse gas flux to the atmosphere, for example, methane that originates from organic matter decomposition in thermokarst lakes. The set of pathways that link methane production in sediments, via oxidation in the lake system, to the flux of residual methane to the atmosphere is complex and exhibits temporal and spatial variation. The isotopic signal of bacterial biomarkers (hopanoids, e.g. diploptene) in sediments has been used to identify contemporary ocean-floor methane seeps and, in the geological record, periods of enhanced methane production (e.g. the PETM). The biomarker approach could potentially be used to assess temporal changes in lake emissions through the Holocene via the sedimentary biomarker record. However, there are no data on the consistency of the signal of isotopic depletion in relation to source or on the amount of noise (unexplained variation) in biomarker values from modern lake sediments. We assessed methane oxidation as represented by the isotopic signal of methane oxidising bacteria (MOB) in multiple surface sediment samples in three distinct areas known to emit varying levels of methane in two shallow Alaskan thermokarst lakes. Diploptene was present and had $\delta^{13}C$ values lower than -38‰ in all sediments analysed, suggesting methane oxidation was widespread. However, there was considerable variation in $\delta^{13}C$ values within each area. The most ^{13}C -depleted diploptene was found in an area of high methane ebullition in Ace Lake (diploptene $\delta^{13}C$ values between -68.2 and -50.1‰). In contrast, significantly less depleted diploptene $\delta^{13}C$ values (between -42.9 and -38.8‰) were found in an area of methane ebullition in Smith Lake. $\delta^{13}C$ values of diploptene between -56.8 and -46.9‰ were found in centre of Smith Lake, where ebullition rates are low but diffusive methane efflux occurs. The small-scale heterogeneity of the samples may reflect patchy distribution of substrate and/or MOB within the sediments. The two ebullition areas differ in age and type of organic carbon substrate, which may affect methane production, transport and subsequent oxidation. Given the high amount of variation in surface samples, a more extensive calibration of modern sediment properties, within and among lakes, is required before down-core records of hopanoid isotopic signatures are developed.

1 Introduction

Arctic lakes are sources of methane within the global carbon cycle (Bastviken 2004). More specifically, thermokarst and thermokarst-affected lakes (those formed and/or influenced by thaw and collapse of ice-rich ground) are recognized as important but variable past and present sources of methane flux to the atmosphere (Shirokova et al., 2012; Walter et al., 2006, 2008; Wik et al., 2013). Predictions of future variation in methane emission rates are largely based on measurements recorded over the last 15 years (e.g. Brosius et al., 2012; Walter Anthony et al., 2014). Long-term (i.e. Holocene) variations in lake-derived methane flux to the atmosphere and changes in emissions during discrete climatic events in the past are generally not well understood (but see Walter Anthony et al., 2014; Walter et al., 2007b). Understanding methane activity in lakes over recent (e.g., decadal/centennial) and longer (millennial) time periods and its relationship with forcing factors (e.g., temperature) could provide useful constraints for the projection of future fluxes with arctic warming.

A significant fraction of methane produced in lake sediments may be oxidized and recycled within the lake by methane oxidising bacteria (MOB), a process that offsets methane emissions (Bastviken et al., 2002; Liebner and Wagner, 2007; Reeburgh, 2007; Trotsenko and Khmelenina, 2005). Methane oxidation (MO) is a critical process for tracking past methane production, as the bacteria that carry it out leave a distinctive trace (biomarkers) in the sediments that were their habitat (see below). However, before this proxy can be developed we need to better understand the link between methane production, MO within the lake system and its geochemical representation, and observed fluxes to the atmosphere. Our study contributes towards this goal by assessing the $\delta^{13}C$ values of bacterial biomarkers obtained from the surficial sediments of two Alaskan lakes to ascertain if i) MO was occurring, and ii) the degree of MO observed in areas characterized by different modes of methane production and transport to the atmosphere.

1.1. Methane processing in thermokarst lakes

Methane production in thermokarst lakes takes two forms: production occurring in anoxic surface sediments, as is common in most freshwater lakes and reservoirs, and that occurring in deeper sediments, especially along the boundary of the "thaw bulb", which is specific to thermokarst lakes (Figure 1). Commonly, methane production occurs via mineralisation of older organic carbon from sources not found in other types of lake: i) where thermokarst-induced erosion leads to large-scale slumping of banks into the littoral zone; material is

typically of Holocene age, but may be older (Figure 1), and ii) the microbial processing of older, labile carbon in the talik, i.e., thawed sediment of the original landscape underlying the lake.

Once produced, methane can be transported to the atmosphere through a number of pathways: ebullition (bubbling), turbulent diffusion and plant mediated transport (Bastviken, 2004). Walter Anthony et al. (2010) postulate that most thermokarst-specific methane production is transported to the atmosphere via seep ebullition. Thermokarst-specific methane ebullition seeps have been studied using GPS mapping and submerged bubble traps and appear to be persistent, spatially explicit fluxes at the water-air interface (Sepulveda-Jauregui et al., 2015; Walter Anthony and Anthony, 2013; Walter et al., 2006, 2008). Spatial stability is attributed to the development of conduits or 'bubble tubes' (Greinert et al., 2010; Scandella et al., 2011), which form point sources at the sediment-water interface. Typically, such seeps are densest near actively eroding lake margins, which we call the "thermokarst zone". Here, methanogenesis is high due to the thermokarst-specific sources of methane production: thawing of fresh talik and bank collapse (Figure 1; Kessler et al., 2012). Less work has focused on methane production in the surficial sediments of thermokarst lakes, its dissolution and diffusion from the sediments to the water column, and the resultant diffusive emission rates. The diffusive flux component can, however, be relatively high, particularly in older, more stable thermokarst lakes that have accumulated Holocene-aged organic carbon in near-surface sediments (Martinez-Cruz et al., 2015; Walter Anthony et al., 2010).

1.2 Determining past methane activity using biomarker proxies

Past methane activity can be addressed qualitatively by using indirect proxies, for example, features related to the cycle of methane through the lacustrine food web. Biogenic methane has highly depleted $\delta^{13}C$ values (usually -80 to -50‰, Whiticar, 1999), depending on the methane production pathway and substrate availability, and this signal can be extracted from various organisms that utilise methane as a food source. Many studies have used the $\delta^{13}C$ values of compounds such as hopanoids from bacteria as indicators of past MO, relating depleted $\delta^{13}C$ values with increased MO and methane supply (e.g. Boetius et al., 2000; Collister and Wavrek, 1996; Hinrichs et al., 2003; Pancost et al., 2007).

The compound diploptene (17 β(H), 21 β(H)-hop-22 (29)-ene), is a hopanoid hydrocarbon derived from a range of bacterial sources including heterotrophs and methanotrophs. Therefore, the $\delta^{13}C$ values of diploptene represent a mixing relationship, with ^{13}C -depleted

MOB at one end and ^{13}C -enriched heterotrophic bacteria (which utilise organic carbon from vegetation) at the other end (Pancost and Sinninghe Damste, 2003 and references therein).

In marine sediments, and especially in microbial mats associated with methane seeps, diploptene has been identified as a methanotrophic biomarker via negative $\delta^{13}C$ values (Elvert et al., 2001b; Pancost et al., 2000a, 2000b). Similarly, it has been argued to have a partial methanotroph source on the basis of low $\delta^{13}C$ values in Holocene peat (Elvert et al., 2001b; Pancost et al., 2000a, 2000b; van Winden et al., 2010; Zheng et al., 2014). Diploptene and the related diplopterol have been used to infer past patterns of MO from marine sediment records (Jahnke et al., 1999; Pancost et al., 2000a) and lake sediments (Spooner et al., 1994).

1.3 Detecting past changes in methane oxidation in thermokarst lakes

If MOB are present in the sediments of thermokarst lakes, we would expect to see depleted $\delta^{13}C$ values of diploptene. To oxidise methane effectively, MOB require access to dissolved methane, and thus it is assumed that MOB-related isotopic depletion indicates oxidation of dissolved methane. However, the strong ebullition observed in some thermokarst lakes complicates the issue, as the relationship between methane that diffuses from sediments (and is either recycled in the lake via MO or released to the atmosphere) and methane that is released to the atmosphere via ebullition remains unclear.

Numerous studies suggest that the methane transport pathways diffusion and ebullition co-vary. In deep marine environments a correlation between methane supply in sediments, transported via either diffusive processes or advectively at cold seeps, and MO as indicated by $\delta^{13}C$ values of specific bacteria and of compounds (Elvert et al., 2001a; Pancost et al., 2001, 2000b). In a shallow (9-m) bight the formation of bubble tubes was linked with increased methane diffusing from the sediments, the proposed explanation being that bubble tubes create an increased surface area that enhances methane diffusion, even though the methane transported via ebullition is taken directly to the atmosphere and is not subject to oxidation (Martens and Klump, 1980).

While little work has focused on MO in thermokarst lakes (but see Martinez-Cruz et al., 2015), He et al. (2012) provide evidence for a possible correlation between a methane ebullition seep (in this case, coal-bed sourced) and MO in a thermokarst lake, L. Qalluuraq, Alaska. Using DNA-based stable-isotope probing they calculated the highest MO potentials near the seep, and these were associated with the presence of MOB in the sediments. This suggests a potential link between methane ebullition and increased availability of methane

that can be utilised by organisms in the lake sediments and water column. However, He et al. (2012) also observed high variability in MO potentials and methanotroph communities with changing substrates, temperature and sediment depth, indicating the need for further investigation of MO in thermokarst lakes. In contrast, based on $\delta^{13}C$ and δD stable isotope values and radiocarbon ages of methane in bubbles, Walter et al. (2008) and Walter Anthony et al. (2014) suggest that methane originating in deep thaw-bulb sediments and emitted by ebullition by-passes aerobic MO and that the majority (90%) of deep-sourced methane is transported through ebullition seeps as opposed to via diffusion. Thus there is currently limited and contrasting evidence for a link or otherwise between levels of methane ebullition and methane diffusion in thermokarst lakes.

2 Regional context & Study sites

Yedoma-like deposits that are similar to those described in Siberia (Schirrmiester et al 2011) can be found in Interior Alaska. In Alaska these sediments can have a relatively high organic content (i.e., retransported silt; Péwé, 1975). They are also rich in excess ice (up to 80% in Siberia). Thermokarst lakes that develop in landscapes dominated by such deposits have been categorized as yedoma lakes in previous studies (Walter et al., 2008; Brosius et al., 2012; Sepulveda-Jauregui et al., 2015). Two lakes were sampled in April 2011 and July 2012 (Figure 2). Ace Lake represents a yedoma lake (Sepulveda-Jauregui et al., 2015), where the sediments surrounding the lake and eroding into it along its NE margin are predominantly yedoma. Smith Lake is classified as a non-yedoma lake in which Holocene-aged deposits are likely the main source of organic matter fuelling methane production.

Smith L. (64°51'55.92"N, 147°52'0.70"W; figure 2) is a shallow (≤4 m), productive lake located near the University of Alaska, Fairbanks. It has a gentle bathymetric profile with average water depths between 1-3m. The lake is not subject to a strong fetch or high energy inflow or outflow. It is eutrophic, and observations during ice-free periods suggest high primary productivity, with blue/green algal blooms predominant throughout the summer months. The lake likely originated by thermokarst processes (Alexander and Barsdate, 1971); comparisons of lake shorelines between the 1950s and today suggest that segments of the southern and western margins have been actively thawing and eroding during recent decades, and tilting trees currently lining the margin of a bay on the southeast shore are further

183 evidence of localized thermokarst. Smith Lake's shallow profile reduces the potential of
184 production or storage of methane due to stratification in the ice-free season.

185 Ace L. (64°51'45.49N, 147°56'05.69W) is part of the Ace-Deuce system (Alexander and
186 Barsdate, 1974) situated within an area covered by the Pleistocene Gold Hill Loess and
187 Goldstream Formation (Péwé, 1975). Ace L. is thermokarst in origin and formed through the
188 thawing of ice bodies in the loess. The Ace-Deuce Lake system has high nutrient levels and
189 can be described as a eutrophic lake with a strong seasonal nutrient cycle (Alexander and
190 Barsdate, 1974). As with Smith L., blue/green algal blooms are common throughout the
191 summer months.

192

193 # 3 Methods

194 ## 3.1 Establishing the thermokarst zones

195 Walter Anthony and Anthony (2013) defined the 'thermokarst' zone for a number of lakes,
196 and we continue to use this definition here, i.e., the region of active thermokarst margin
197 expansion observed using historical aerial photographs obtained during the past 60 years. In
198 most lakes, the density of ebullition seeps is higher in thermokarst zones compared to
199 elsewhere (Walter Anthony and Anthony, 2013). In Ace and Smith Lakes, ebullition
200 emission rates have been quantitatively monitored through a combination of early-winter ice-
201 bubble surveys and bubble-trap flux measurements in previous studies (see Sepulveda-
202 Jauregui et al., 2015 for methods). We obtained surface sediment cores, from both the ice and
203 open water well within the zone boundaries and as close to observed ebullition seep locations
204 as possible (figure 2). The deepest part of Ace L. (the central area) was not sampled. The
205 development of a thermocline and anoxic bottom waters in deeper sections of Ace L. would
206 likely have an effect on both the rate of production and oxidation of methane that occurs in
207 the surface sediments. Eliminating such factors reduces the number of variables which might
208 explain the $\delta^{13}C$ values derived in this study.

209 ## 3.2 Methane monitoring

210 Ebullition gas samples were collected from seep locations (October 2009 at Smith L and
211 April, 2011 at Ace L.) in the thermokarst zone (n1 and n5 for Smith L, and Ace L.
212 respectively) in the manner described in Walter Anthony et al. (2012) for determination of

bubble methane concentration and stable isotope analyses. Gases were collected from submerged bubble traps into 60-ml glass serum vials following Walter et al. (2008), sealed with butyl rubber stoppers, and stored under refrigeration in the dark until analysis in the laboratory. We measured methane concentration using a Shimadzu 2014 equipped with an FID at the Water and Environmental Research Centre at University of Alaska Fairbanks (UAF). We determined $\delta^{13}C_{CH4}$, using a Finnegan Mat Delta V at Florida State University. Subsamples of gas were combusted to CO_2, purified, and catalytically reduced to graphite (Stuiver and Polach, 1977), and the $^{13}C/^{12}C$ isotopic ratios were measured by accelerator mass spectrometry at the Woods Hole Oceanographic Institution's National Ocean Sciences AMS Facility. Stable isotope compositions are expressed in δ (‰) = 103 (($R_{sample}/R_{standard}$)-1), where R is $^{13}C/^{12}C$ standard refers to the Vienna Pee Dee Belemnite (VPDB). The analytical error of the stable isotopic analysis was ± 0.1 ‰ $\delta^{13}C$. We express radiocarbon data as percent modern carbon pmC (%) = (($^{14}C/^{12}C)_{sample}/(^{14}C/^{12}C)$standard) x 100, which is the percentage of $^{14}C/^{12}C$ ratio normalized to $\delta^{13}C$ = -25‰ and decay corrected relative to that of an oxalic standard in 1950 (Stuiver and Polach, 1977).

3.3 Biomarker analysis

Surface sediment samples were retrieved using a gravity corer and the 0-5cm sequence was extruded at 1-cm resolution and retained for analysis; the 1-2 cm slice was subsampled for biomarker analysis and not the top as the sediment-water interface was often difficult to sample cleanly due to unconsolidated sediments. The 1-2 cm slice integrates a number of years of sediment accumulation (>10years) which reflects samples from a palaeoenvironment. Two sequential sediment extractions were performed to obtain the total lipid extract. The first step was a modified Bligh and Dyer extraction (Bligh and Dyer, 1959). Briefly, buffered water was prepared adjusting a solution of 0.05M KH_2PO_4 in water to pH 7.2 through the addition of NaOH pellets. Subsequently, a monophasic solvent mixture was made up with buffered water, $CHCl_3$ and MeOH (4:5:10 v/v). Samples were sonicated in Bligh-Dyer solvent mixture for 15 minutes and then centrifuged at 3000 rpm for 5 minutes. Supernatant was collected in a round bottom flask. This step was repeated twice and all supernatants were combined and dried to obtain the total lipid extraction (TLE) labelled TLE1. Post-extraction sediment residues were air-dried. The Bligh and Dyer post-extraction residues were sonicated in DCM for 15 minutes and then centrifuged at 3000 rpm for 5 minutes. This step was repeated first with DCM:MeOH (1:1, v/v) and then with MeOH.

Supernatants were combined after every step of sonication-centrifugation to obtain TLE2. Both TLE1 and TLE2 were then combined to yield the final TLE.

The TLE was split into three fractions of increasing polarity using silica flash column chromatography (Oba et al., 2006; Pitcher et al., 2009). Silica gel columns (0.5 g, 60 Å particle size) were prepared and conditioned with 4 ml of *n*-hexane:ethyl acetate (3:1, v/v). Fractions were eluted with 3 ml of *n*-hexane:ethyl acetate (3:1, v/v) to obtain the simple lipid fraction, 3 ml of ethyl acetate to obtain glycolipids and 10ml of MeOH to obtain phospholipids. The simple lipid fraction was further split into neutral lipid and the fatty acid fractions. The organic phase was then collected into a round bottom flask and Na_2SO_4 anhydrous was added until complete removal of water. Silica gel columns (again, 0.5 g, 60 Å particle size) were prepared and conditioned with 4 ml of the recently prepared $CHCl_3$ sat solution. The simple lipid fraction was then loaded onto the column and subsequently, the neutral lipid fraction was eluted with 9 ml of $CHCl_3$ sat. Finally, the neutral lipids were separated into apolar and polar lipid fractions. Columns were prepared with approximately 0.5 g of activated alumina (Al_2O_3) and compounds eluted with 4 ml of *n*-hexane:DCM (9:1, v/v) and 3 ml of DCM:MeOH (1:2, v/v) to yield the two fractions, respectively. Here, we focus on analyses of the neutral lipid apolar fraction as this is the fraction where diploptene will elute.

3.4 Compound identification and Compound-specific $\delta^{13}C$ isotope analysis

GC-MS analyses were performed using a Thermoquest Finnigan Trace GC and MS. The GC was fitted with an on-column injector and the stationary phase was CP Sil5-CB. Detection was achieved with electron ionization (source at 70 eV, scanning range 50-580 Daltons). The temperature program consisted of three stages: 70-130 °C at 20 °C/min rate; 130-300 °C at 4 °C/min; and 300 °C, temperature held for 10 min.

Gas chromatography combustion isotope ratio mass spectrometry (GC-IRMS) was performed using a ThermoScientific Trace GC Ultra coupled to a Conflo IV interface and DeltaV mass Spectrometer. The GC conditions and program were the same as for GC-MS analyses. Calibration was achieved using CO_2 reference gas of known isotopic composition and sample $\delta^{13}C$ values were expressed against the standard VPDB. All measurements were performed in duplicate.

3.5 Mass Balance equation

A carbon isotopic mass balance equation (Equation 1), or two-part mixing model, was developed to evaluate the contribution of MOB to the total bacterial biomass, and, therefore, the relative amount of oxidation occurring at each sample location. By developing this mixing model and considering in more detail the potential end member values for the $\delta^{13}C$ values of diploptene derived from different sources (MOB and other heterotrophic bacteria) we can obtain a semi-quantitative estimation of the distribution patterns of MOB across the samples.

The resulting end member values are given in table 1. The equation is as follows:

$$f_{mob} = \frac{\delta^{13}C_{dip\_sample} - \delta^{13}C_{hetero\_dip}}{\delta^{13}C_{mob\_dip} - \delta^{13}C_{hetero\_dip}} \quad (1)$$

Where f_{mob} is the fraction of diploptene generated by MOB and $\delta^{13}C_{dip\_sample}$ is the stable carbon isotopic composition of diploptene in a given sample. $\delta^{13}C_{hetero\_dip}$ and $\delta^{13}C_{mob\text{-}dip}$ are the inferred $\delta^{13}C$ values of diploptene if it were derived solely from heterotrophic bacteria and methanotrophic bacteria, respectively. Both are expressed as the $\delta^{13}C_{bacterial\_biomass} - \Delta^{13}C_{biosynthesis}$, the latter term reflecting fractionation during biosynthesis of diploptene.

For heterotrophs, it is likely that $\delta^{13}C_{bacterial\_biomass}$ is similar to that of the substrate organic carbon and is calculated from the $\delta^{13}C_{bulk\_sediment}$ taken in each zone of the lake. For heterotrophic bacteria, $\Delta^{13}C_{biosynthesis}$ can vary from ~2 to 8‰ or more (Pancost and Sininnghe Damsté 2003, and references therein) and a representative value of 4‰ is used here. Given the small range in $\Delta^{13}C_{biosynthesis}$ and $\delta^{13}C_{bulk\_sediment}$ values, the minimum and maximum values for $\delta^{13}C_{hetero\_dip}$ are similar.

For MOB, $\delta^{13}C_{bacterial\_biomass}$ is calculated from the $\delta^{13}C_{methane}$ minus the fractionation that occurs during carbon uptake by methanotrophs (0-30‰; Jahnke et al., 1999). The $\delta^{13}C_{methane}$ is the measured value of methane captured at seep locations in the thermokarst zones at each lake. As the value is based on a limited number of data points (n=1 and n=5 for Smith L. and Ace L. respectively), it is likely there will be more variation than is seen in the model. In order to incorporate the large range for fractionation that occurs during carbon uptake by methanotrophs (Jahnke et al., 1999), we used both the minimum and maximum value of fractionation (0 and 30‰) to show different scenarios rather than assuming a single value. This is likely larger than variation due to differing $\delta^{13}C_{methane}$. With little information available on the fractionation of hopanoids during their biosynthesis by MOB, we assumed a

306 conservative value of 10‰ for our study. This is larger than value assigned for heterotrophic
307 bacteria but still remains a realistic estimate. We calculated mass balances based on both the
308 maximum and minimum end member $\delta^{13}C$ values for heterotroph- and methanotroph-derived
309 diploptene.

310

311 # 4 Results

312 ## 4.1 Methane signatures

313 Early-winter ice-bubble surveys, combined with bubble-trap measurements of ebullition flux
314 and bubble methane concentration, revealed that ebullition seeps occur with high density in
315 the thermokarst zones of both lakes (2.27 seeps m^2 and 4.2 seeps m^2 for Smith L. and Ace L.,
316 respectively as estimated from ice-bubble surveys) compared to the rest of the lake (0.35
317 seeps m^2 and 0.67 seeps m^2 for Smith L. and Ace L., respectively).

318 Seep ebullition rates in the thermokarst zones were 85 and 151 mg CH_4 m^{-2} d^{-1} for Smith L.
319 and Ace L., respectively (Figure 2). In the rest of each lake (lake centre and non-thermokarst
320 margins) seep ebullition rates were 6 and 20 mg CH_4 m^{-2} d^{-1} for Smith L. and Ace L.,
321 respectively. The $\delta^{13}C$ values for methane in bubbles collected from seeps in the thermokarst
322 zones were -60.9‰ and -64.6‰ for Smith Lake and Ace L., respectively.

323 ## 4.2 Dipoloptene $\delta^{13}C$ values

324 Diploptene was detected in all but one of the samples analysed (Table 2; figure 3). The
325 isotopic values ranged from -68.2 to -38.8‰ and had an overall standard deviation of 7.8‰.

326 In the Ace L. thermokarst zone, diploptene values ranged from the lowest value for the whole
327 dataset of -68.2 to -50.1‰. Both the most negative and least negative values were found at
328 the greatest water depth (3.2m) in samples located very close to one another, suggesting high
329 variability across small spatial scales.

330 In Smith L., diploptene $\delta^{13}C$ values ranged from -56.8 to -38.8‰. The most negative value
331 was found in the centre of the lake, and the difference between this and the least negative
332 value (-46.9‰) in the centre of the lake is almost 10‰. In the Smith L. thermokarst zone
333 there was less variability in diploptene $\delta^{13}C$ (-42.9 to -38.8‰); however, there is still a
334 difference in values of 4.1‰. Samples from the centre of the lake and the thermoakrst zone
335 (n=6, n=3 respectively) were compared using a Mann-Whiney U test (H0: diploptene $\delta^{13}C$

values are not different). The test suggested a significant difference between samples from the centre and the thermokarst zone suggesting a difference in bacterial community composition.

A comparison of both thermokarst zones shows that diploptene $\delta^{13}C$ values at Ace L. were more negative than those at Smith L. by at least 10‰. The samples in the thermokarst zone of Ace L. and the centre of Smith L. (n=4, n=6 respectively) were not significantly different according to a Mann Whitney U test.

4.3 Mixing model predictions

The potential contributions of MOB to the diploptene signal under different end-member assumptions are shown in Table 3. The minimum and maximum contributions range from 19 to 85%, 7 to 27% and 19 to 63% for Ace L. thermokarst zone, Smith L. thermokarst zone and Smith centre, respectively.

Ace L. thermokarst zone had the highest overall potential contributions but also the largest range of predicted values. Smith L. centre had the second highest contribution of MOB to the diploptene signal, and, apart from one sample, suggested a more consistent contribution across the zone. Smith L. thermokarst zone had the lowest potential contribution of the total dataset; even when choosing end member values that yield the greatest MOB contribution, values only reached 27%.

5 Discussion

Ace L. thermokarst zone had the highest observed ebullition emission rates, the most depleted $\delta^{13}C$ diploptene values and the highest potential MOB contribution (according to the mixing model results). The highest ebullition emission rates in Smith L. were in the thermokarst zone, which had the lowest MOB contributions and least depleted $\delta^{13}C$ diploptene values. The centre of Smith L. had very low ebullition rates but depleted $\delta^{13}C$ diploptene values and high predictions of MOB contributions.

The $\delta^{13}C$ diploptene signatures are similar to those that have been previously highlighted as evidence for methanotrophy in lacustrine sediments (-64‰ to -55‰; Spooner et al., 1994; Naeher et al., 2014), marine sediments (-62‰ to -35‰; Freeman et al., 1994; Thiel et al., 2003) and wetlands (-40‰ to -30‰ to; van Winden et al., 2010; Zheng 2014). Therefore, we conclude that diploptene $\delta^{13}C$ values are documenting the presence of at least some MOB

bacteria in lake sediments. The lowest values in Ace L. are among the lowest reported for lacustrine (or other terrestrial) systems, suggesting a relatively high degree of methanotrophy at those sampling sites. Moreover, although the diploptene values were highly variable, the highest values yielded MOB fractions >10%, even when using the most conservative assumptions (Table 3).

The results of the mixing model suggest that MOB can contribute anywhere between 7-83% of the diploptene production across all sampled areas (Table 3). These estimates have a large degree of uncertainty and we note that there are some important caveats to using this mixing model. Crucially, diploptene is not derived from all bacteria nor even all methanotrophic bacteria (Rohmer et al., 1987). Nor is it likely to occur in constant biomass-to-lipid ratios in those organisms from which it can derive. Thus, using a diploptene mass balance to infer bacterial biomass distributions should be done cautiously, and the data should be considered semi-quantitative. Nonetheless, a MOB contribution to total biomass of ~10 to 80% is similar to that derived from other studies (11-80%; Bastviken et al. 2003; Sundh et al. 2005; Kankaala et al. 2006). Regardless of absolute MOB estimates, our data show that the centre of Smith L. and the thermokarst zone at Ace L. likely have the highest proportion of MOB in the total bacterial biomass.

At Ace L., MOB biomass was high relative to other samples collected in this study and in the context of previous studies. Ace L. has been classified as a 'yedoma-type' lake in previous studies (Walter et al., 2008; Sepulveda-Jauregui, et al., 2015; see above). Walter Anthony and Anthony (2013) suggest that yedoma thermokarst lakes typically produce more methane than non-yedoma thermokarst lakes owing to a higher availability of labile carbon in thick, thawed yedoma sequences. Given the coincidence of high ebullition emission rates, depleted $\delta^{13}C$ diploptene signatures and high estimated MOB biomass, it is likely that the supply of dissolved methane is high in the thermokarst zone and that this methane might be derived from thermokarst-specific sources. Alternatively, lake-edge thermokarst erosion of yedoma-type sediments is also known to supply nitrogen and phosphorus to lakes (Walter Anthony et al. 2014), enhancing primary production, which in turn can fuel methanogenesis and MO from contemporary (atmospheric) carbon (Martinez-Cruz et al., 2015).

Within the thermokarst zone at Smith L. the $\delta^{13}C$ values of diploptene were less variable than in the Ace L. thermokarst zone, and the $\delta^{13}C$ values were more enriched. In fact, the thermokarst zone in Smith L. had the lowest proportion of MOB for the entire dataset, with a MOB contribution to diploptene being near-equivocal for most of these samples, with values

at or below 10% according to the mixing model. On the other hand, despite evidence for much lower methane efflux, samples from the centre of Smith L. had diploptene $\delta^{13}C$ values that were similar to those of the Ace L. thermokarst zone. The differences between the centre and the thermokarst zone in Smith L. could be explained by several processes. They could arise from variation in the microbial community that is manifest as different MOB expressions of hopanoids. For example, the thermokarst zone MOB might not be biosynthesising diploptene or its precursor. Alternatively, there may be differences in the balance of MO contributing to energy versus biomass production in the bacterial community. Another explanation, which could be validated through further investigation, relates to potential differences in methane production pathways, as highlighted by Walter et al. (2008). In this case, the higher $\delta^{13}C$ values of diploptene in the thermokarst zone could be due to more enriched methane formed through acetate fermentation. However, the most direct interpretation of the data is that MOB are more abundant in the centre of the lake than at the thermokarst margin and, by extension, more MO is taking place in the lake centre.

Overall, the Smith L. thermokarst zone had lower methane ebullition rates and less negative $\delta^{13}C$ of methane as measured from ebullition flux than Ace L. Therefore, compared with Ace L., the availability of methane produced in this the Smith L. thermokarst zone may be lower due to physical differences in substrate organization. At Smith L. it is likely that methane is not produced in the talik but in near-surface sediments related to peat slumping at the margin. The large size of the sediment blocks and the early stage of decomposition of the slumped organic material may mean there is less exposed substrate surface area for methane production, as compared with yedoma-lake production from fine-grained and more labile talik sediments. Also, methane production in near-surface sediments (often linked to shallow water depths) is subject to reduced partial pressure and faster release of bubbles from the sediment. Bubble tubes initiated in sediments shallower than the talik bulb are likely to be reduced in overall number and size.

An important outcome of this study is the large degree of variation seen in the $\delta^{13}C$ values of diploptene across small spatial distances. The variation does not clearly correspond to patterns in methane production (e.g. high and low ebullition areas). In fact, in Smith L, diploptene $\delta^{13}C$ values are lower in the low methane flux lake centre than in the high flux thermokarst zone. Despite the caveats associated with interpreting diploptene $\delta^{13}C$ values, the difference is so large that it likely does indeed reflect more MO in the lake centre. We suggest that this is due to more efficient MO in some diffusive settings than in some

433 thermokarst settings, where ebullition may effectively bypass the MO community. Regardless
434 of mechanism, this variability is a significant finding, as often whole-lake dynamics are
435 interpreted from a single sediment core in palaeoenvironmental studies. Such large variation
436 in $\delta^{13}C$ values in surface sediments taken from the same zone within a lake – as well as the
437 complex relationships between inferred MO and methane flux – highlight the need for
438 caution when interpreting shifts in $\delta^{13}C$ values through time using down-core values.

439 Interestingly, a previous study of MOB in lake sediments also reported considerable variation
440 in bacterial communities at small spatial scales (Kankaala et al., 2006). High spatial and/or
441 temporal variability in MOB and other elements of the bacterial biomass could also affect the
442 isotopic composition of heterotrophs higher in the food web, if they consume MOB (e.g.,
443 chironomid larvae). This could have implications for interpretation of not only biomarkers
444 but also other geochemical records. For example, investigations of the biological and
445 geochemical connections between MOB and isotopic signatures of organisms at higher
446 trophic levels are needed, if such organisms are used to interpret past methane emissions.

447 While the results of this study show the potential of diploptene $\delta^{13}C$ signatures to highlight
448 MO in lakes, further work is needed to understand what this signature is reflecting in terms of
449 methane production and flux. Whether there is a positive correlation between ebullition flux
450 and high diffusion in the thermokarst zone is still to be determined. The current data show no
451 clear link. While this is one of very few studies to use within-lake replicates, and differences
452 are statistically significant, the sample number is small and the system could usefully be
453 tested further prior to developing down-core studies.

454

455 ## 6 Conclusions

456 Our primary goal was to contribute towards the understanding of the sedimentary signature of
457 methane production and oxidation in thermokarst lakes using diploptene $\delta^{13}C$ values as a
458 proxy for the occurrence of MOB. Diploptene was present in almost all samples, and the
459 $\delta^{13}C$ values were depleted, suggesting the presence of MOB in three zones with differing
460 levels of methane ebullition emissions rates. A two-part mixing model highlighted the
461 potential variation in total MOB biomass, with almost no MOB contributing to bacterial
462 biomass in some samples but forming over half the total bacterial population in others.
463 Critically, these $\delta^{13}C$ values were highly variable within zones, suggesting small-scale spatial
464 heterogeneity in MOB abundance and thus methane oxidation. The data do not show a

consistent relationship between MOB abundance and methane emission rates at the lake surface; in fact, in Smith L, it appears that high MOB abundance occurs where methane emissions are low, suggesting that pathways of carbon flow are as or more important than total flux. Therefore, further investigation of the different types of methane ebullition observed in thermokarst lakes, the relationship between these and diffusion and the different expression of these pathways and MOB biomass are critical. There is also a need to examine localized spatial variability of MO within lakes and how any spatial variation is integrated temporally, as this may critically affect observed down-core patterns of biomarkers and their isotopic signals.

Acknowledgements

This research was supported by a NERC grant (NE/K000233/1) to M. Edwards and P. Langdon, a QRA new researcher's award to K. Davies and a PhD Scholarship to K. Davies from Geography and Environment, University of Southampton. We gratefully acknowledge field and equipment assistance from Nancy Bigelow, Charlotte Clarke, Rob Collier and Ben Gaglioti, and permission from the owners to work at Ace Lake. Mark Dover (Cartography Unit, G&E) made valuable improvements to the figures.

References

Alexander, V. and Barsdate, R. J.: Physical Limnology, Chemistry and Plant Productivity of a Taiga Lake, Int. Rev. ges. Hydrobiol, 56(6), 825–872, 1971.

Alexander, V. and Barsdate, R. J.: Limnological Studies of a Subarctic Lake System, Int. Rev. ges. Hydrobiol, 59(6), 737–753, 1974.

Bastviken, D.: Methane emissions from lakes: Dependence of lake characteristics, two regional assessments, and a global estimate, Global Biogeochem. Cycles, 18(4), GB4009, doi:10.1029/2004GB002238, 2004.

Bastviken, D., Ejlertsson, J., Sundh, I. and Tranvik, L.: Methane as a source of carbon and energy for lake pelagic food webs, Ecology, 84(4), 969–981, doi:10.1890/0012-9658(2003)084[0969:MAASOC]2.0.CO;2, 2003.

Bligh, E. G. and Dyer, W. J.: A rapid method of total lipid extraction and purification, Can. J. Biochem. Physiol., 37(8), 911–917, 1959.

Boetius, A., Ravenschlag, K., Schubert, C. J., Rickert, D., Widdel, F., Gieseke, A., Amann, R., Jorgensen, B. B., Witte, U. and Pfannkuche, O.: A marine microbial consortium apparently mediating anaerobic oxidation of methane, Nature, 407(6804), 623–626 [online] Available from: http://dx.doi.org/10.1038/35036572, 2000.

Collister, J. W. and Wavrek, D. A.: δ13C compositions of saturate and aromatic fractions of lacustrine oils and bitumens: evidence for water column stratification, Org. Geochem., 24(8–9), 913–920, doi:http://dx.doi.org/10.1016/S0146-6380(96)00066-6, 1996.

Elvert, M., Greinert, J., Suess, E. and Whiticar, M. J.: Carbon Isotopes of Biomarkers Derived from Methane Oxidizing Microbes at Hydrate Ridge, Cascadia Convergent Margin, Nat. Gas Hydrates Occur. Distrib. Detect., 115–129, 2001a.

Elvert, M., Whiticar, M. . and Suess, E.: Diploptene in varved sediments of Saanich Inlet: indicator of increasing bacterial activity under anaerobic conditions during the Holocene, Mar. Geol., 174(1-4), 371–383, doi:10.1016/S0025-3227(00)00161-4, 2001b.

Freeman, K. H., Wakeham, S. G. and Hayes, J. M.: Predictive isotopic biogeochemistry: hydrocarbons from anoxic marine basins., Org. Geochem., 21(6-7), 629–44, 1994.

Greinert, J., Lewis, K. B., Bialas, J., Pecher, I. a., Rowden, a., Bowden, D. a., De Batist, M. and Linke, P.: Methane seepage along the Hikurangi Margin, New Zealand: Overview of studies in 2006 and 2007 and new evidence from visual, bathymetric and hydroacoustic investigations, Mar. Geol., 272(1-4), 6–25, doi:10.1016/j.margeo.2010.01.017, 2010.

He, R., Wooller, M. J., Pohlman, J. W., Quensen, J., Tiedje, J. M. and Leigh, M. B.: Shifts in identity and activity of methanotrophs in arctic lake sediments in response to temperature changes., Appl. Environ. Microbiol., 78(13), 4715–23, doi:10.1128/AEM.00853-12, 2012.

Hinrichs, K.-U., Hmelo, L. R. and Sylva, S. P.: Molecular Fossil Record of Elevated Methane Levels in Late Pleistocene Coastal Waters, Science (80-.)., 299(5610), 1214–1217 [online] Available from: http://science.sciencemag.org/content/299/5610/1214.abstract, 2003.

Jahnke, L. L., Summons, R. E., Hope, J. M. and Des Marais, D. J.: Carbon isotopic fractionation in lipids from methanotrophic bacteria II : The effects of physiology and environmental parameters on the biosynthesis and isotopic signatures of biomarkers, Geochim. Cosmochim. Acta, 63(1), 79–93, 1999.

Kankaala, P., Huotari, J., Peltomaa, E., Saloranta, T. and Ojala, A.: Methanotrophic activity in relation to methane efflux and total heterotrophic bacterial production in a stratified, humic, boreal lake, Limnol. Oceanogr., 51(2), 1195–1204, doi:10.4319/lo.2006.51.2.1195, 2006.

Kessler, M. a., Plug, L. J. and Walter Anthony, K. M.: Simulating the decadal- to millennial-scale dynamics of morphology and sequestered carbon mobilization of two thermokarst lakes in NW Alaska, J. Geophys. Res. Biogeosciences, 117(G2), n/a–n/a, doi:10.1029/2011JG001796, 2012.

Martens, C. P. S. and Klump, J. V. A. L.: Biogeochemical cycling in an organic-rich coastal marine basin-I . Methane sediment-water exchange processes, Geochim. Cosmochim. Acta, 44, 471–490, 1980.

Martinez-Cruz, K., Sepulveda-Jauregui, A., Walter Anthony, K. and Thalasso, F.: Geographic and seasonal variation of dissolved methane and aerobic methane oxidation in Alaskan lakes, Biogeosciences Discuss., 12(5), 4213–4243, doi:10.5194/bgd-12-4213-2015, 2015.

Naeher, S., Niemann, H., Peterse, F., Smittenberg, R. H., Zigah, P. K. and Schubert, C. J.: Tracing the methane cycle with lipid biomarkers in Lake Rotsee (Switzerland), Org. Geochem., 66, 174–181, doi:10.1016/j.orggeochem.2013.11.002, 2014.

Oba, M., Sakata, S. and Tsunogai, U.: Polar and neutral isopranyl glycerol ether lipids as biomarkers of archaea in near-surface sediments from the Nankai Trough, Org. Geochem., 37(12), 1643–1654, 2006.

Pancost, R. ., Hopmans, E. . and Sinninghe Damsté, J. .: Archaeal lipids in Mediterranean cold seeps: molecular proxies for anaerobic methane oxidation, Geochim. Cosmochim. Acta, 65(10), 1611–1627, doi:10.1016/S0016-7037(00)00562-7, 2001.

Pancost, R. D., Damsté, J. S. S., De, S., Maarel, M. J. E. C. Van Der and Gottschal, J. C.: Biomarker Evidence for Widespread Anaerobic Methane Oxidation in Mediterranean Sediments by a Consortium of Methanogenic Archaea and Bacteria, Appl. Environ. Microbiol., 66(3), 1126–1132, doi:10.1128/AEM.66.3.1126-1132.2000.Updated, 2000a.

Pancost, R. D., Geel, B. Van, Baas, M. and Sinninghe Damsté, J. S.: d13C values and radiocarbon dates of microbial biomarkers as tracers for carbon recycling in peat deposits, Geology, 28(7), 663–666, doi:10.1130/0091-7613(2000)28<663, 2000b.

Pancost, R. D., Steart, D. S., Handley, L., Collinson, M. E., Hooker, J. J., Scott, A. C., Grassineau, N. V and Glasspool, I. J.: Increased terrestrial methane cycling at the Palaeocene-Eocene thermal maximum, Nature, 449(7160), 332–335 [online] Available from: http://dx.doi.org/10.1038/nature06012, 2007.

Péwé, T. L.: Quaternary geology of Alaska, 1975.

Pitcher, A., Hopmans, E. C., Schouten, S. and Damsté, J. S. S.: Separation of core and intact polar archaeal tetraether lipids using silica columns: insights into living and fossil biomass contributions, Org. Geochem., 40(1), 12–19, 2009.

Reeburgh, W. S.: Oceanic methane biogeochemistry., Chem. Rev., 107(2), 486–513, doi:10.1021/cr050362v, 2007.

Scandella, B. P., Varadharajan, C., Hemond, H. F., Ruppel, C. and Juanes, R.: A conduit dilation model of methane venting from lake sediments, Geophys. Res. Lett., 38(6), n/a–n/a, doi:10.1029/2011GL046768, 2011.

Sepulveda-Jauregui, a., Walter Anthony, K. M., Martinez-Cruz, K., Greene, S. and Thalasso, F.: Methane and carbon dioxide emissions from 40 lakes along a north–south latitudinal transect in Alaska, Biogeosciences, 12(11), 3197–3223, doi:10.5194/bg-12-3197-2015, 2015.

Shirokova, L. S., Pokrovsky, O. S., Kirpotin, S. N., Desmukh, C., Pokrovsky, B. G., Audry, S. and Viers, J.: Biogeochemistry of organic carbon, CO2, CH4, and trace elements in

584 thermokarst water bodies in discontinuous permafrost zones of Western Siberia,
585 Biogeochemistry, 113(1-3), 573–593, doi:10.1007/s10533-012-9790-4, 2012.

586 Spooner, N., Rieley, G., Collister, J. W., Lander, I. M., Cranwell, I. P. A. and Maxwell, J. R.:
587 Stable carbon isotopic correlation of individual biolipids in aquatic organisms and a lake
588 bottom sediment, Org. Geochem., 21(6/7), 823–827, 1994.

589 Stuiver, M. and Polach, H. A.: Discussion; reporting of C-14 data., Radiocarbon, 19(3), 355–
590 363, 1977.

591 Sundh, I., Bastviken, D. and Tranvik, L. J.: Abundance, activity, and community structure of
592 pelagic methane-oxidizing bacteria in temperate lakes, Appl. Environ. Microbiol., 71(11),
593 6746–6752, 2005.

594 Thiel, V., Blumenberg, M., Pape, T., Seifert, R. and Michaelis, W.: Unexpected occurrence
595 of hopanoids at gas seeps in the Black Sea, Org. Geochem., 34(1), 81–87,
596 doi:10.1016/S0146-6380(02)00191-2, 2003.

597 Walter Anthony, K. M. and Anthony, P.: Constraining spatial variability of methane
598 ebullition seeps in thermokarst lakes using point process models, J. Geophys. Res.
599 Biogeosciences, 118(July), 1015–1034, doi:10.1002/jgrg.20087, 2013.

600 Walter Anthony, K. M., Vas, D. A., Brosius, L., Iii, F. S. C., Zimov, S. A. and Zhuang, Q.:
601 Estimating methane emissions from northern lakes using ice- bubble surveys, Limnol.
602 Oceanogr. Methods, 8, 592–609, 2010.

603 Walter Anthony, K. M., Zimov, S. a, Grosse, G., Jones, M. C., Anthony, P. M., Chapin, F. S.,
604 Finlay, J. C., Mack, M. C., Davydov, S., Frenzel, P. and Frolking, S.: A shift of thermokarst
605 lakes from carbon sources to sinks during the Holocene epoch., Nature, 511(7510), 452–6,
606 doi:10.1038/nature13560, 2014.

607 Walter, K. M., Zimov, S. A., Chanton, J. P., D., V. and Chapin III, F. S.: Methane bubbling
608 from Siberian thaw lakes as a positive feedback to climate warming., Nature, 443(7107), 71–
609 5, doi:10.1038/nature05040, 2006.

610 Walter, K. M., Smith, L. C. and Chapin, F. S.: Methane bubbling from northern lakes: present
611 and future contributions to the global methane budget., Philos. Trans. A. Math. Phys. Eng.
612 Sci., 365(1856), 1657–76, doi:10.1098/rsta.2007.2036, 2007a.

613 Walter, K. M., Edwards, M. E., Grosse, G., Zimov, S. A. and Chapin, F. S.: Thermokarst
614 lakes as a source of atmospheric CH4 during the last deglaciation., Science, 318(5850), 633–
615 6, doi:10.1126/science.1142924, 2007b.

616 Walter, K. M., Chanton, J. P., Chapin, F. S., Schuur, E. a. G. and Zimov, S. a.: Methane
617 production and bubble emissions from arctic lakes: Isotopic implications for source pathways
618 and ages, J. Geophys. Res., 113, doi:10.1029/2007JG000569, 2008.

619 Whiticar, M. J.: Carbon and hydrogen isotope systematics of bacterial formation and
620 oxidation of methane, Chem. Geol., 161(1-3), 291–314, doi:10.1016/S0009-2541(99)00092-
621 3, 1999.

622 Wik, M., Crill, P. M., Varner, R. K. and Bastviken, D.: Multiyear measurements of ebullitive
623 methane flux from three subarctic lakes, J. Geophys. Res. Biogeosciences, 118(April), n/a–
624 n/a, doi:10.1002/jgrg.20103, 2013.

625 van Winden, J. F., Kip, N., Reichart, G.-J., Jetten, M. S. M., Camp, H. J. M. O. Den and
626 Damsté, J. S. S.: Lipids of symbiotic methane-oxidizing bacteria in peat moss studied using
627 stable carbon isotopic labelling, Org. Geochem., 41(9), 1040–1044,
628 doi:10.1016/j.orggeochem.2010.04.015, 2010.

629 Zheng, Y., Singarayer, J. S., Cheng, P., Yu, X., Liu, Z., Valdes, P. J. and Pancost, R. D.:
630 Holocene variations in peatland methane cycling associated with the Asian summer monsoon
631 system., Nat. Commun., 5, 4631, doi:10.1038/ncomms5631, 2014.

632

633

634

635

636

637

638

639

640

641

642

643

644

645

646

647

648

649

650

651

652

653

654 Table 1. Mixing model end member values and $\delta^{13}C$ values of the primary variables used to
655 calculate the proportion of MOB at each sample point. $\delta^{13}C_{bulk}$ is the average bulk sediment

value from each lake, ± indicates the standard deviation of the $\delta^{13}C_{bulk}$. MOB and heterotrophic bacteria have been assumed to have maximum levels of lipid biosynthesis occurring (10 and 4‰ respectively). $\delta^{13}C_{mob\_dip\_min}$ is the estimated minimum stable isotope value given the $\delta^{13}C$ value of methane at each lake and the maximum potential fractionation of carbon by MOB. $\delta^{13}C_{mob\_dip\_max}$ is the estimated value of MOB with no fractionation during assimilation. $\delta^{13}C_{hetero\_dip\_max}$ is the maximum estimated stable isotope value of heterotrophic bacteria if no fractionation is occurring during assimilation and the bulk sediment is +1.0 standard deviation (S.D.) from the mean at each lake. $\delta^{13}C_{hetero\text{-}hopane\_min}$ represents the minimum value for heterotrophic hopanes given maximum possible fractionation during assimilation and if bulk sediment is -1.0 S.D from the mean.

	$\delta^{13}C_{bulk}$ (‰)	n	±	$\delta^{13}C_{mob\_dip\_min}$ (‰)	$\delta^{13}C_{mob\_dip\_max}$ (‰)	$\delta^{13}C_{hetero\_dip\_min}$ (‰)	$\delta^{13}C_{hetero\_dip\_max}$ (‰)
Ace	-30.8	10	2.1	-104.6	-74.6	-36.9	-32.7
Smith	-29.3	10	0.8	-100.9	-70.9	-34.1	-32.5

Table 2 $\delta^{13}C$ values of diploptene at the study sites. The values are an average of three replicates. The standard deviation of these replicates and of each zone and across all samples is also given.

		Sample Number	$\delta^{13}C_{dip}$ (‰)	Sample replicate standard Deviation (SD)		Standard Deviation (SD)
Ace						
	TK zone	a1	-50.1	1.5		
		a2	-58.5	2.0		
		a3	-53.1	0.4		
		a4	-68.2	0.1	TK zone	8.0
Smith						
	Centre	1	-51.4	2.7		
		2	-48.3	0.0		
		3	-56.8	N/A		
		4	-49.2	1.0		
		5	-46.9	1.8		
		6	-48.0	0.1	Centre	3.6
	TK zone	7	-38.8	0.3		
		8	-40.9	0.2		
		9	-42.9	0.1		
		10	N/A	N/A	TK zone	2.0
					Total	7.8

Table 3. Estimated contribution of MOB to the diploptene signal. Calculations assume fractionation due to biosynthesis of 10‰ for MOB and 4‰ for heterotrophic bacteria. f_{mob_min} was calculated assuming the highest fractionation for both MOB and heterotrophs (30 and 4‰ respectively). f_{mob_max} assumes no fractionation during assimilation. $f_{mob\_average}$ was calculated using average $\delta^{13}C$ values for $\delta^{13}C_{mob\text{-}hopane}$ and $\delta^{13}C_{hetero\text{-}hopane}$.

		Sample Number	f_{mob_min}	f_{mob_max}	$f_{mob\_average}$
Ace					
	TK zone	a1	0.19	0.42	0.28
		a2	0.32	0.62	0.43
		a3	0.24	0.49	0.33
		a4	0.46	0.85	0.61
Smith					
	Centre	1	0.26	0.49	0.34
		2	0.21	0.41	0.28
		3	0.34	0.63	0.45
		4	0.23	0.44	0.30
		5	0.19	0.37	0.26
		6	0.21	0.40	0.28
	TK zone	7	0.07	0.17	0.11
		8	0.10	0.22	0.14
		9	0.13	0.27	0.18

Figure 1. Illustration of methane production zones and emission pathways in lakes alongside thermokarst-specific zones and pathways. 1) Surface sediment ebullition zone (background methane production). Methane that is produced in the anoxic surface sediments is released via ebullition, usually near the margins (Bastviken et al., 2004). (2) Surface sediment diffusion zone. Methane is produced in the anoxic surface sediments and diffuses in the sediments above and into the water column. Some of this methane will reach the water surface-air interface but a large amount is likely to be oxidised by MOB (Kankaala et al., 2006). This process is common in many lakes also. (3) Talik zone. Methane is produced in the deeper talik sediments underneath the lake and is released via ebullition seeps (Walter et al. 2008). Often this is a higher flux and is more constant than surface sediment ebullition. This production zone and pathway is a thermokarst-specific process. (4) Slump zone. Methane production in the surface sediments is increased due to the introduction of large volumes of slumped sediments. This methane is also released via ebullition seeps. Often, the flux from these ebullition seeps is higher than surface sediment ebullition but not as high as talik ebullition. This process might occur in any lakes that have dynamic margins and high erosion rates; however, it is likely that this process is most common in thermokarst lakes due to the melting of permafrost, so it is termed thermokarst-specific. Red question marks indicate where methane diffusion from the sediments has not been studied in detail.

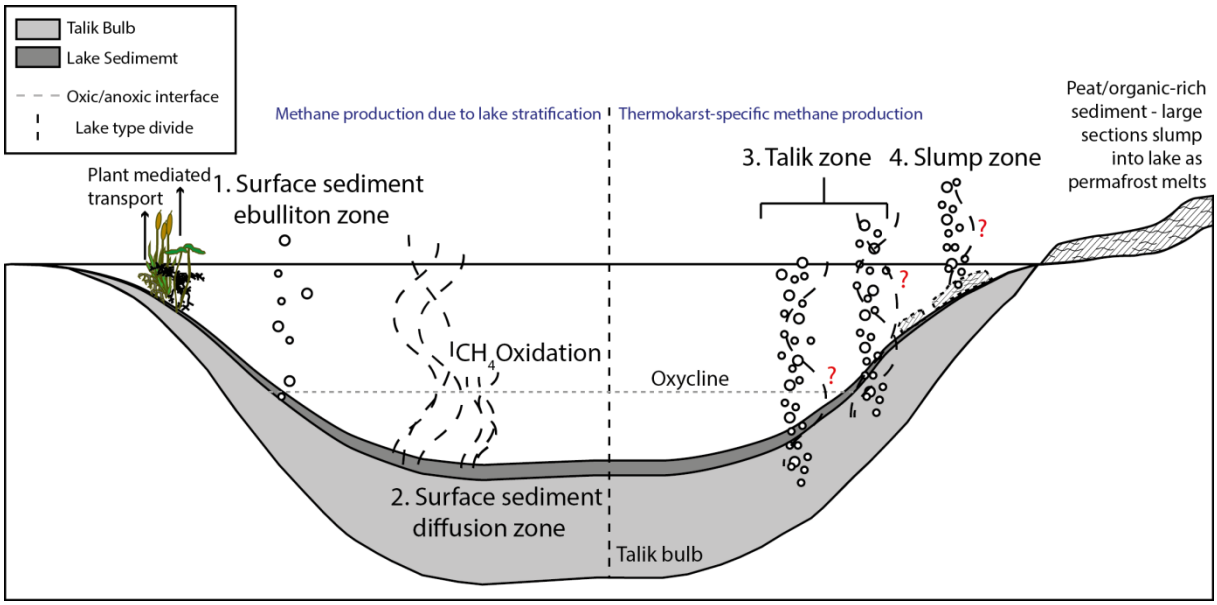

Figure 2. Locations of the study lakes in Alaska and the sediment sample points within each lake. The red (Ace L.) and blue (Smith L.) bars indicate the flux values as averaged within a given area of the lake. Flux measurements were taken on October 2009 at Smith L and April, 2011 at Ace L.

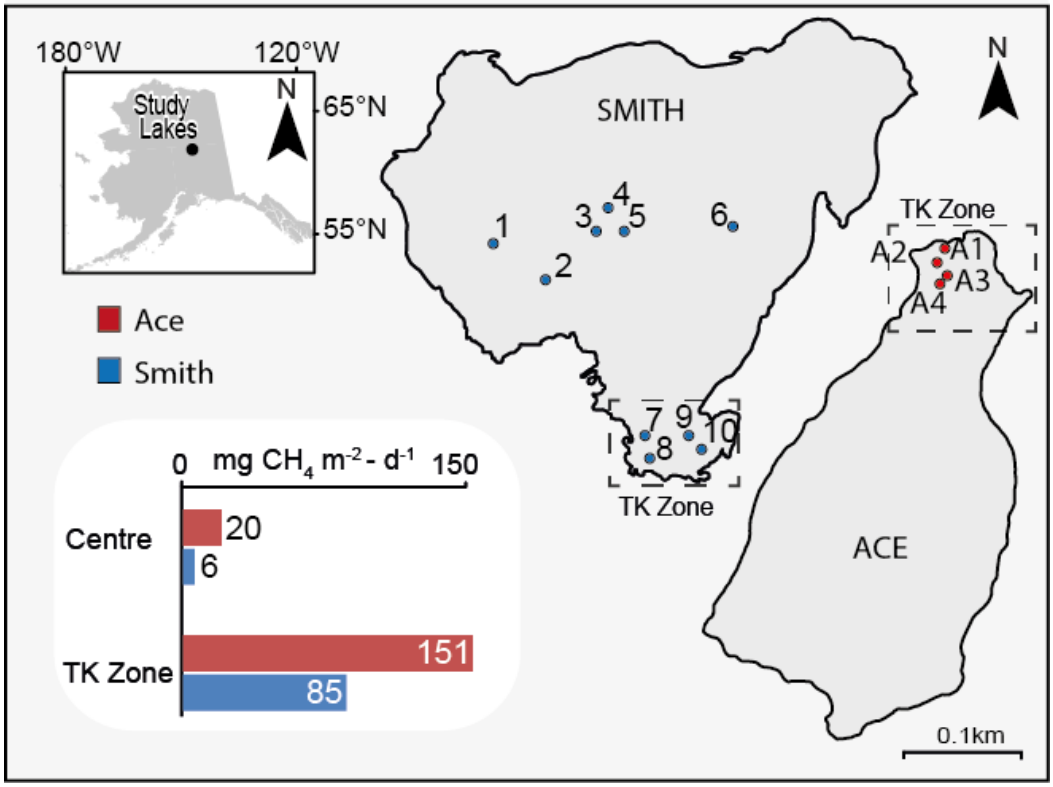

Figure 3. Diploptene $\delta^{13}C$ values at Smith Lake and Ace Lake. In general the most depleted values are found in Ace and in the centre of Smith. The Thermokarst zone at Smith L. has the least depleted values for the whole dataset